PHYSICAL REVIEW A VOLUME 44, NUMBER 6 15 SEPTEMBER 1991

Measurements of the gas kinetic temperature in a CH_4-H_2 discharge during the growth of diamond

H. N. Chu
Physics Department, University of Wisconsin, Madison, Wisconsin 53706

E. A. Den Hartog
Engineering Research Center for Plasma-Aided Manufacturing,
University of Wisconsin, Madison, Wisconsin 53706

A. R. Lefkow
Department of Material Science and Engineering,
University of Wisconsin, Madison, Wisconsin 53706

J. Jacobs
Engineering Research Center for Plasma-Aided Manufacturing,
University of Wisconsin, Madison, Wisconsin 53706

L. W. Anderson
Physics Department, University of Wisconsin, Madison, Wisconsin 53706

M. G. Lagally
Department of Material Science and Engineering,
University of Wisconsin, Madison, Wisconsin 53706

J. E. Lawler
Physics Department, University of Wisconsin, Madison, Wisconsin 53706

(Received 8 April 1991)

Experiments to study the gas kinetic temperature in a dc hollow cathode discharge have been carried out under conditions suitable for diamond growth using CH_4-H_2 mixtures as the feed gas. The gas kinetic temperature is shown to be equal to the rotational temperature for particular emission bands in H_2 and in CN in a CH_4-H_2 discharge containing a small N_2 impurity for total pressures above 10 Torr. The gas temperature can be obtained by measuring relative line intensities in emission of either the R branch of the $G\,{}^1\Sigma_g^+ \rightarrow B\,{}^1\Sigma_u^+(0\text{-}0)$ band of H_2 or the R branch of the $B\,{}^2\Sigma^+ \rightarrow X\,{}^2\Sigma^+(0\text{-}0)$ band of CN. The (0-0) symbol represents a band of transitions occurring between the levels with 0 vibrational quantum number in the upper electronic state and the levels with 0 vibrational quantum number in the lower electronic state. These measurements of gas kinetic temperature in a CH_4-H_2 discharge using optical emission spectroscopy have been confirmed by two different experiments using laser-induced fluorescence.

I. INTRODUCTION

It is well known that diamond has a number of properties that are or may be useful in scientific and industrial applications. In the past few years, various methods for the deposition of diamond from the gas phase using chemical-vapor deposition (CVD) have been reported. Plasma-assisted CVD (PACVD) using discharges containing CH_4-H_2 mixtures is one of the most commonly used techniques for the deposition of diamond films [1–4]. For both the growth rate and quality of the diamond films the optimum substrate temperature is between 1100 and 1300 K [5–7]. It is likely that the deposition process is also sensitive to the gas kinetic temperature. The gas temperature helps determine the concentration of various radicals, because many gas-phase reaction rates are strongly dependent on the gas kinetic temperature. Consequently, diagnostic techniques that determine the gas temperature are important.

The glow-discharge plasmas used in diamond deposition usually have neutral gas densities in the range 10^{18} cm^{-3} and have electron densities many orders of magnitude lower. Although these discharges operate far from local thermodynamic equilibrium, there are degrees of freedom that equilibrate. The relative population of rotational levels in a long-lived electronic vibrational level of a diatomic molecule is well described by a Boltzmann distribution with T_r, the rotational temperature, equal to T, the gas kinetic temperature. Virtually every gas kinetic collision changes the rotational quantum number, while collisions that change the electronic or vibrational quantum number are much less frequent. The rotational distribution in short-lived electronic vibrational levels may be or may not be equilibrated depending on the relative size of rotational redistribution rates versus total quenching rates, and depending on how far the initial distribution is from rotational thermal equilibrium.

We have identified emission bands in both H_2 and CN that have T_r equal to T under typical diamond growing conditions. The bands are also optically thin, strong, and not seriously blended with other features in the rich emission spectrum from the discharge. The use of optical emission spectroscopy (OES) on these bands provides a simple, inexpensive technique for measuring T. We have used laser-induced fluorescence (LIF) on the long-lived ground electronic vibrational level of CN to confirm that T_r from the emission band is equal to T. We have also used LIF to study rotational redistribution in the $B\ ^2\Sigma^+$ of CN.

II. DIAMOND FILM DEPOSITION

A schematic diagram of our apparatus is shown in Fig. 1. The hollow cathode, which is made of tantalum, is similar to that described in Ref. [4]. A feed gas mixture of CH_4 and H_2 flows through the hollow cathode, inside of which an intense discharge decomposes the feed gases so that the gas emerging from the hollow cathode contains a wide variety of molecules and free radicals. During the growth of diamond, the hollow cathode becomes white hot (about 1900 °C) and the discharge is extremely stable. The spacing between the cathode and the anode is 2.5 cm. The anode is made of p-type (100) Si. It is 4 cm in length and 1 cm in width. The anode is heated by passing an ac current through it. The anode temperature can be varied independently of other deposition processing parameters and is measured with an optical pyrometer. The anode to cathode voltage is typically 250 V and the discharge current is typically 1 A. A typical total gas flow rate is 40 SCCM (where SCCM denotes cubic centimeter per minute at STP). A typical diamond film growth rate is 2 μm/h. That diamond rather than diamondlike carbon is being grown, is determined both by observing the diamond crystals using a scanning electron microscope and by observing the Raman scattering of diamond at 1332 cm^{-1}. Diamond films have been deposited for the gas mixtures of CH_4 in H_2 ranging from 0.5% to 1% by volume, and for total gas pressures ranging from 10 to 90 Torr.

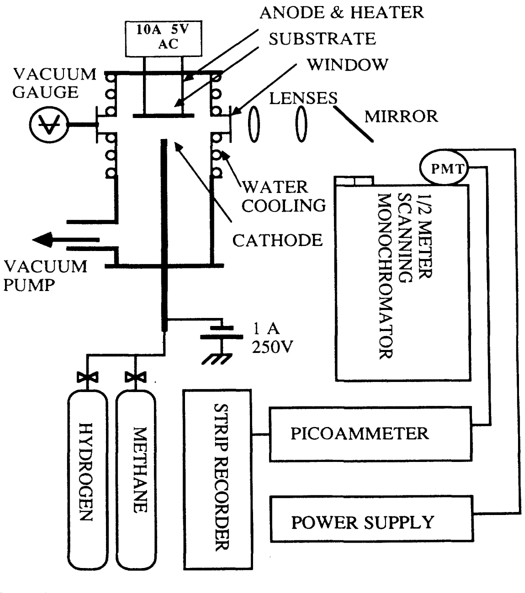

FIG. 1. Schematic diagram of the PACVD deposition system.

III. GAS TEMPERATURE MEASURED USING OPTICAL EMISSION SPECTROSCOPY

A half meter monochromator with a spectral resolution of 0.03 nm is used to observe the emission spectrum of the discharge. Light from a region of the discharge parallel to the anode is collected and focused using $f/6$ optics onto the entrance slit of the monochromator. All measurements are integrations along the line of sight. The density of molecules or radicals and the temperature may vary along the line of sight. The emission spectrum from 350 to 700 nm has been studied. The observed spectrum shows many atomic lines and molecular bands. The H_α, H_β, and H_γ lines are very intense and easily recognized. The wavelength calibration of the monochromator is determined from the prominent H_α, H_β, and H_γ lines and by easily identified lines from a low-pressure Hg lamp. Numerous electronic bands of H_2 and CN have been identified. The CN bands result from a low concentration of N_2 in the CH_4 feed gas.

The relative emission intensities of rotational lines in a large number of electronic bands of the H_2 molecule [8] have been studied. The R branch lines of the $G\ ^1\Sigma_g^+ \rightarrow B\ ^1\Sigma_u^+$(0-0) band of H_2 at 462.8 nm is shown in Fig. 2. It is found that a plot of ln (I/S) for this band is a linear function of the upper rotational energy under a variety of conditions except for the $R6$ and $R9$ components. Here, I is the relative intensity of the emission divided by the nuclear spin degeneracy in order to take into account the symmetry properties of the rotational levels [9]. The line strengths S are equal to $J'+J''+1$ in emission where J' and J'' are the rotational quantum numbers of the upper and lower levels, respectively. The R branch is the series of lines corresponding to $J'-J''=+1$ transition. Figure 3 shows a typical Boltzmann plot of ln (I/S) for the R branch of the $G\ ^1\Sigma_g^+ \rightarrow B\ ^1\Sigma_u^+$(0-0) band as a function of the energy of the upper levels. $R1$–$R4$ are omitted from

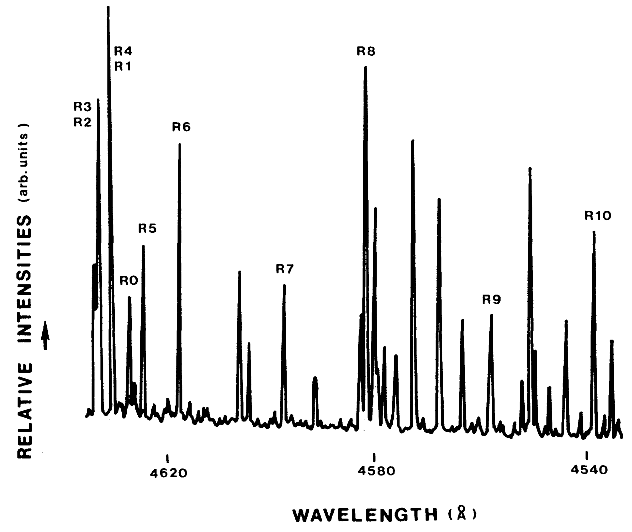

FIG. 2. Spectra of the R branch of the $G\,^1\Sigma_g^+ \rightarrow B\,^1\Sigma_u^+$(0-0) band of the H_2 molecule.

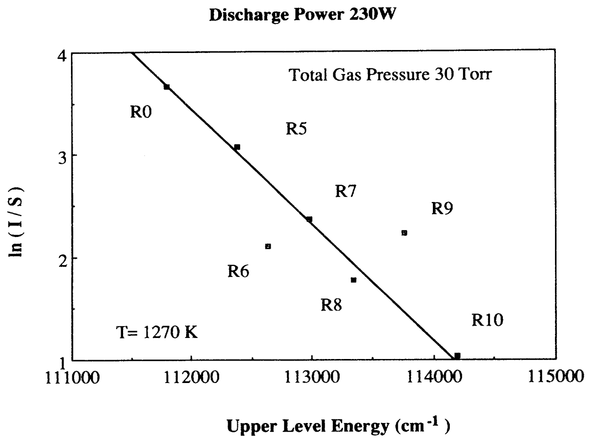

FIG. 3. Rotational temperature obtained using emission intensities divided by the nuclear spin degeneracy of the H_2 molecule at 30-Torr total pressure with CH_4:$H_2$$=1\%$ by volume. $S=J'+J''+1$. Data were taken at a position 12.5 mm above the cathode.

the plot because they are not individually resolved from one another in the emission spectrum. It is important to note that upper level energies and wavelengths in this band are not described by standard formulas because of perturbations from other nearby H_2 levels [10]. A potential problem is that the various upper rotational levels may be so seriously perturbed by nearby levels that there are different lifetimes for the different rotational levels. Even for the R branch of the $G\,^1\Sigma_g^+ \rightarrow B\,^1\Sigma_u^+(0\text{-}0)$ band the $R6$ line consistently lies 27% below the straight line on the plots of the ln (I/S) as a function of the energy of the upper level, which is probably caused by such a perturbation. The $R9$ line always lies high on the plots of the ln (I/S) as a function of the energy of the upper level. The $R9$ line has a larger width than the other lines, which is a good indication that it is blended with one or more other lines. The $R9$ line is therefore omitted from the data fitting.

All of the other electronic bands of the H_2 molecule that have been studied are either seriously perturbed or are not well resolved in the spectrum, so that a plot of natural log of intensity as a function of the rotational energy of the upper levels is not a straight line. Because most bands in H_2 are perturbed, a second unperturbed emission band has been sought so that the derived temperatures can be compared in order to determine whether the straight line plot of the ln (I/S) for the R branch of the $G\,^1\Sigma_g^+ \rightarrow B\,^1\Sigma_u^+(0\text{-}0)$ band as a function of the rotational energy of the upper level results from a rotational thermal equilibrium or from some accidental conditions.

In our CH_4-H_2 discharge, we have observed CN electronic emission bands resulting from a N_2 impurity in CH_4. The R branch of the $B\,^2\Sigma^+ \rightarrow X\,^2\Sigma^+(0\text{-}0)$ band of CN at 388.3 nm [Ref. 11] has been investigated. This well-studied "violet" band of CN is known to have only slight perturbations, and has previously been used for rotational temperature measurements [9]. Because of the small spacing between adjacent rotational energy levels, the half meter monochromator was used with an echelle grating operating in the 14th order with an instrument resolution of 0.008 nm to resolve the rotational lines in the CN band. A narrow-band interference filter with 10-nm bandpass at 386 nm was used to isolate a single order of the echelle grating . After eliminating lines that are obviously blended as indicated by wider line shapes than for other lines, it is found that a plot of ln (I/S) as a function of the energy of the upper rotational levels of the CN band has a slope that gives nearly the same temperature as a measurement taken under the same conditions using the H_2 band. The $B\,^2\Sigma^+ \rightarrow X\,^2\Sigma^+(0\text{-}0)$ band of CN belongs to the Hund's case (b) in which a doublet splitting appears and increases linearly with K. In general K is the sum of the electronic orbital and molecular rotational angular momentum. In this case K is the appropriate quantum number instead of J and the line strengths S are equal to $K'+K''+1$. We have neglected spin-rotational splitting in our analysis because it is not resolved in our spectra. Figure 4 shows a Boltzmann plot for the temperature measured using relative emission line intensities from the R branch of the $B\,^2\Sigma^+ \rightarrow X\,^2\Sigma^+(0\text{-}0)$ band of CN. The CN emission measurements were taken using the same discharge condition and spatial position as for the H_2 emission measurements shown in Fig. 3.

There are several potential problems with a determination of the gas kinetic temperature using relative emission intensities of rotational lines within an electronic band. The first problem is that there must be enough collisions to assure that the rotational population reflects the gas kinetic temperature. The radiative decay rate of the upper level of the $G\,^1\Sigma_g^+ \rightarrow B\,^1\Sigma_u^+(0\text{-}0)$ H_2 band is 3×10^7 s^{-1} [12]. Using a collisional cross section radius 2.93 Å of Gallagher and Fenn [13] the collision rate of gas molecules is estimated to be 2×10^8 s^{-1} at a total pressure of 30 Torr and at gas temperature 1200 K. Therefore it is believed that the collisional rate is large enough that the rotational temperature in the excited electronic state is equal to the gas kinetic temperature. Another potential

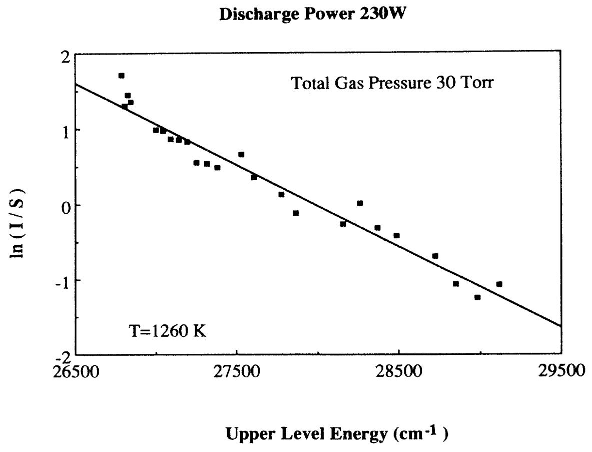

FIG. 4. Rotational temperature obtained using emission intensities of the CN molecule at 30-Torr total pressure with CH_4 : $H_2$$=1\%$ by volume. $S=K'+K''+1$. Data were taken at a position 12.5 mm above the cathode.

problem is the optical depth. Self-absorption is a potential source of systematic error in this type of measurement. The $B\ ^1\Sigma_u^+$ level of the H_2 band has a short radiative lifetime. It does not have sufficient population to produce self absorption of the H_2 band.

There are convincing reasons that the rotational temperature obtained from the CN emission is equal to the gas kinetic temperature. They are the following: (a) the radiative decay rate of the $B\ ^2\Sigma^+$ level is $1.5\times10^7\ s^{-1}$ [14], which is sufficiently small that at pressures above 10 Torr Jackson and Cody [15] find there are enough collisions to equilibrate the rotational energy levels, (b) the CN band unlike the H_2 band is relatively unperturbed, because it is between low-lying electronic levels, and (c) although the CN band is connected to the ground electronic level, it is optically thin because CN is a minor impurity in our system. This was verified by intentionally leaking dry nitrogen into the system. With the nitrogen leak, the discharge produces about 30 times more CN emission than without the leak. Even under this condition the absorption of a nonsaturating laser tuned to the band head is less than 10%. This result shows clearly that CN is optically thin and that self-absorption is not a problem in our system. The rotational temperature measured from relative line intensities of emission from the R branch of the $G\ ^1\Sigma_g^+ \to B\ ^1\Sigma_u^+(0\text{-}0)$ band of H_2 and emission from the R branch of the $B\ ^2\Sigma^+ \to X\ ^2\Sigma^+(0\text{-}0)$ band of CN are the same within the accuracy of our measurements. This strongly suggests that both the emission band in H_2 and in CN yield a rotational temperature that is equal the gas kinetic temperature.

IV. LASER-INDUCED FLUORESCENCE DETERMINATION OF GAS TEMPERATURE

In order for thermal equilibrium to exist in an excited molecular level, it is necessary that the gas density be high enough that there are sufficient collisions during the lifetime of the excited levels. For a ground-level molecule there are certainly enough collisions at a pressure of 10-Torr or higher to establish a rotational thermal equilibrium so that the rotational populations reflect the gas kinetic temperature. Although the rotational temperature observed in the excited levels of H_2 and CN are the same, it is desirable to measure also the rotational temperature of the ground level of a molecule and hence the gas kinetic temperature in order to provide additional confirmation that the OES measurements represent a true gas kinetic temperature. To determine the ground-level rotational population distribution in CN, we have used laser-induced fluorescence on CN. The ground electronic level CN molecules in a given rotational level are excited using a narrow band dye laser. The laser is scanned to excite different rotational levels sequentially. The fluorescence from all the rotational levels in the excited electronic level is detected. Many excited rotational levels are populated even though a narrow band dye laser is used because once a particular excited level is populated collisions redistribute the population to a large number of rotational levels.

A pulsed nitrogen laser-pumped dye laser with a repetition rate of 50 Hz and pulse duration of 4 ns was used to excite the CN radical on the $v''=0$ to $v'=0$ transition from the ground electronic level to the $B\ ^2\Sigma^+$ level. The wavelength of the excitation laser was scanned through the R branch to excite sequentially the CN radical from many different rotational levels. The laser beam passes horizontally through the center of the discharge about 1 mm above the hollow cathode. This is the same region of the discharge that was sampled using OES. The LIF was collected and focused with $f/5$ optics directly onto a 1P28A photomultiplier, amplified, and integrated with a boxcar integrator. A 70-ns wide gate opens 7 ns after each laser pulse. An interference filter with 10-nm bandpass at 386 nm was used to isolate the LIF light from broadband background light from the discharge. To obtain the signal, a running average over 300 laser shots was performed as the laser was scanned. A small amount of dry nitrogen is leaked into the system to enhance the LIF signal-to-noise ratio. The nitrogen leak rate is so adjusted that the ratio of the intensity of ${N_2}^+$ band head at 391.4 nm to the intensity of the CN band head is 1:80 in emission. The ${N_2}^+$ band at 391.4 nm is the $B\ ^2\Sigma^+ \to X\ ^2\Sigma^+(0\text{-}0)$ band [16]. Because of the large intensity ratio the CN band has only slight blending in emission from the nearby ${N_2}^+$ band at 388.4 nm corresponding to the transition from $v''=1$ to $v'=1$ [16]. In LIF, the possibility for band blending is even smaller than in emission because the ${N_2}^+$ band at 388.4 nm corresponds to a vibrationally excited lower level with $v''=1$. With the nitrogen leak, no absorption due to the 391.4 nm ${N_2}^+$ band has been observed even under optimum signal-to-noise condition. The laser power is adequate to pump the CN radical in the saturated regime as has been tested by inserting neutral density filters in the laser beam before it enters the discharge and observing no change in the fluorescence. The linearity of the photomultiplier is verified by inserting neutral density filters in the collecting optics.

To determine a rotational temperature, the wavelength of the excitation laser is scanned to sequentially excite many different lines in the R branch of the CN radical. Since the width of the observed lines is primarily determined by the laser bandwidth, which is 0.005 nm, the relative peak heights of the LIF signal are used for the Boltzmann plot. Figure 5(c) shows a plot of $\ln(I/S)$ against the energy of the lower rotational levels for the CN band probed with LIF. The LIF line strengths S are equal to $(2K''+1)(K''-1)/(2K''-1)$ for the case where the transitions from the lower level are saturated by the laser and where the fluorescence of the R branch is collected. A concise form [17] of the line strength is used in the Boltzmann plot because neither R-formed Q branches nor P-formed Q branches [18] have been observed. It is noted that the energy of the lower levels instead of the upper levels is used in the Boltzmann plot for the LIF measurements, because lower levels are probed using LIF. Figure 5 shows the comparison of Boltzmann plots of gas temperature measured using relative line intensities from (a) emission from the R branch of the $G\ ^1\Sigma_g^+ \to B\ ^1\Sigma_u^+(0\text{-}0)$ band of H_2, (b) emission from the R branch of the $B\ ^2\Sigma^+ \to X\ ^2\Sigma^+(0\text{-}0)$ band of CN, and (c)

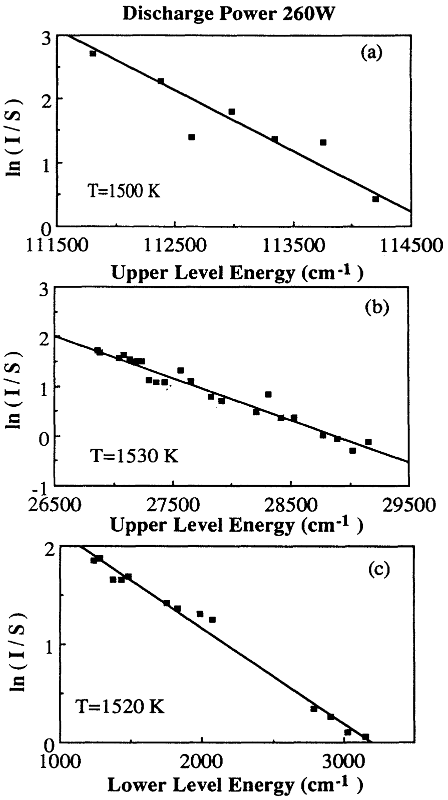

FIG. 5. Comparisons of rotational temperature obtained under the same conditions using relative emission intensities of (a) the H_2 molecule $S=J'+J''+1$, (b) the CN molecule, $S=K'+K''+1$, and (c) LIF of the CN molecule, $S=(2K''+1)(K''-1)/(2K''-1)$. The total pressure was 45 Torr with $CH_4 : H_2=2\%$ by volume. Data were taken at a position 1 mm above the cathode.

LIF of the R branch of the $B\,^2\Sigma^+ \rightarrow X\,^2\Sigma^+(0\text{-}0)$ band of CN, at the same discharge condition and spatial position.

The uncertainty of the measured gas temperature arising from the deviation of the data points from the fitted line for each of the three measurements is smaller than that arising from the long-term reproducibility of the measurements. Therefore, the uncertainty of each measurement is determined from the long-term reproducibility of the measurements. The uncertainties are (a) 5% in using H_2 emission, (b) 6% in using CN emission, and (c) 8% in using the LIF of the CN radical to obtain the gas temperature. The temperatures are the same within these experimental uncertainties. The LIF measurements give the largest experimental uncertainty of the gas temperature because each LIF scan takes two and half hours to finish, and the uncertainty reflects the drift of both instruments and plasma. If a reticon array was used to obtain the gas temperature using relative line intensities from emission from the R branch of the $G\,^1\Sigma_g^+ \rightarrow B\,^1\Sigma_u^+(0\text{-}0)$ band of H_2, then a real time measurement with very small uncertainty should be possible.

The LIF measurements, shown in Fig. 5, indicate that the ground level has the same rotational temperature as the excited level. Figure 6 is a plot of the gas rotational temperature obtained from the R branch of the $G\,^1\Sigma_g^+ \rightarrow B\,^1\Sigma_u^+(0\text{-}0)$ band of H_2 emission, the $B\,^2\Sigma^+ \rightarrow X\,^2\Sigma^+(0\text{-}0)$ band of CN emission, and LIF of the R branch of the $B\,^2\Sigma^+ \rightarrow X\,^2\Sigma^+(0\text{-}0)$ band of CN against the total gas pressure. These indicate that the rotational temperature is equal to the gas kinetic temperature. Since there are good reasons to rely on the measurements of a gas kinetic temperature using CN emission or LIF and since the temperature obtained from H_2 is the same as from CN either in emission or using LIF, we believe that the measurements on the H_2 band also represent a gas kinetic temperature. This is important, since the H_2 band can be observed in any discharge containing H_2 plus a hydrocarbon, whereas the CN band depends on the existence of nitrogen as an impurity.

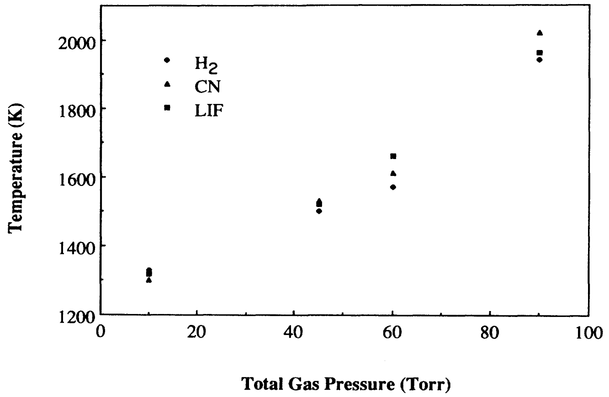

FIG. 6. Gas temperature measured for various total pressures with $CH_4 : H_2=2\%$ by volume. Data were taken at a position 1 mm above the cathode.

V. REDISTRIBUTION TEST USING THE LASER-INDUCED FLUORESCENCE MEASUREMENTS

As a final confirmation that there are a sufficient number of collisions during the lifetime of an excited level to produce rotational thermal equilbrium, we have carried out a LIF experiment where the laser, tuned to two overlapping P branch transitions, pumps CN molecules into two excited rotational levels and emission from excited rotational levels is spectrally resolved. The laser is not scanned in this experiment. Since only two rotational levels are excited by the pump laser our observation of the fluorescence from other levels is a direct measurement of rotation changing collisions between the excited molecule and other gas molecules. This experiment is a very clear demonstration of the collisional redistribution that establishes a rotational equilibrium in the excited level.

Once a radical has been excited, it can spontaneously radiate to a lower level, it can be collisionally quenched to a different vibronic level, or it can make a collision that causes a change of rotational level within the same electronic vibrational level. The excited rotational levels will have a thermal population distribution if enough rotation changing collisions occur during the lifetime of the excited level.

The same laser setup discussed in Sec. IV is used for this experiment, except for the LIF collection system and except that the laser wavelength is not scanned. The wavelength of the excitation laser is fixed to excite the CN radical using two particular lines in the *P* branch of the $B^2\Sigma^+ \rightarrow X^2\Sigma^+(0\text{-}0)$ band of CN. The *P* branch corresponds to $J'-J''=-1$ transitions. The LIF is collected and focused with *f*/6 optics onto the entrance slit of the half meter monochromator. The half meter monochromator was used with an echelle grating operating in the 14th order with an instrument resolution of 0.04 nm. The light is detected with a 1P28A photomultiplier, amplified, and integrated using a boxcar integrator. In order to obtain a signal, a running average over 1000 laser shots is performed. This makes a datum acquisition time 20 s at a 50 Hz laser pulse repetition rate. The band-pass of the monochromator is scanned through the R branch of the CN band with a 0.000 48 nm/s scanning rate. The total length of time for the monochromator bandpass to scan through the instrument resolution is 21 s.

Figure 7 shows a LIF spectrum of the *R* branch of the $B^2\Sigma^+ \rightarrow X^2\Sigma^+(0\text{-}0)$ band of CN when transitions from the rotational levels with $J''=16$ and $J''=40$ in the lower level are saturated by the excitation laser. Two levels rather than one are pumped because they have essentially the same absorption wavelength. The transition lines *P*16 and *P*40 are blended [19] and correspond to excitation of the upper levels of *R* 14 and *R* 38 respectively.

There is the possibility that the fluorescence might arise from a weak wide band dye laser component due to amplified spontaneous emission. If the laser wavelength is detuned away from the wavelength of the transition lines *P*16 and *P*40, the *R* branch transitions do not appear in the fluorescence light spectrum. This indicates that amplified spontaneous emission does not contribute to the transitions in this redistribution test.

As can be seen in Fig. 7 the *R* branch lines with the upper level populated directly by the laser show excess populations over the populations of the other nearby levels. We interpret this as being due to a competition between quenching and the rotational redistribution due to collisions. The excess intensity in the two levels divided by the total intensity of all lines indicates that more than 95% of the excited molecules have undergone one or more rotation changing collisions during the lifetime of the excited level. Figure 8 is a plot of the lower bound of the redistribution ratio against total gas pressure. It shows that the excited levels are well redistributed before they radiate. Since this redistribution ratio is independent of the gas pressure from 30 to 90 Torr, we infer that quenching rather than radiation dominates the lifetime of the excited molecules. The high rates of rotational redistribution are not surprising. In an early experiment of this type Evenson and Broida observed rapid rotational redistribution of CN molecules in the $B^2\Sigma^+$ level due to both He and N_2 collisions [20]. Their results indicate that redistribution ratios of about 90% can be achieved at 10-Torr. A peculiar observation for which we have no satisfactory explanation is the small excess of population in $J'=27$, which corresponds to the band head in the P branch. If we change the pump frequency to correspond to different upper levels then those levels show excess populations rather than the upper levels of *R* 14 and *R* 38 but the level at the band head always shows a small excess population.

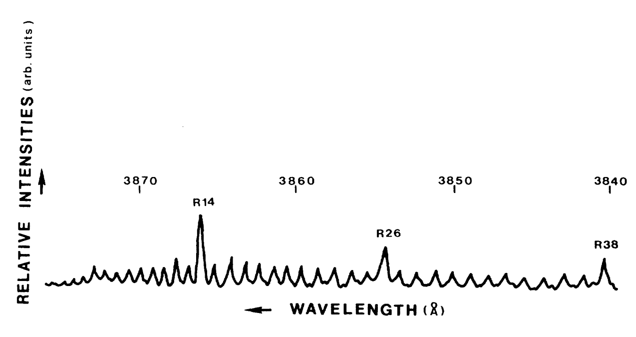

FIG. 7. LIF spectrum of the *R* branch in the $B^2\Sigma^+ \rightarrow X^2\Sigma^+(0\text{-}0)$ band of CN when the *P*16 and *P*40 transitions are saturated by the excitation laser. The total pressure was 60 Torr with $CH_4:H_2=2\%$ by volume. Data were integrated between anode and cathode.

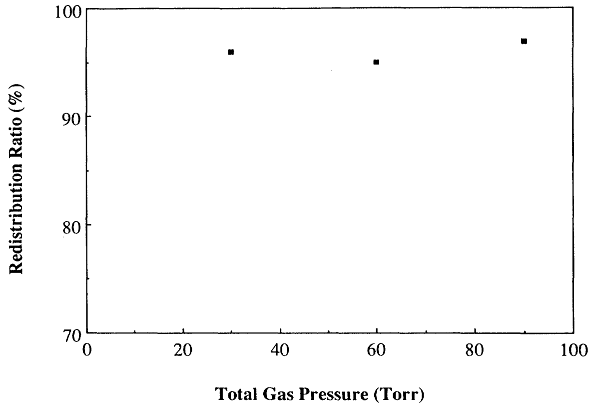

FIG. 8. Plot of the redistribution ratio of the *R* branch in the $B^2\Sigma^+ \rightarrow X^2\Sigma^+(0\text{-}0)$ band of CN as a function of the total pressure with $CH_4:H_2=2\%$ by volume, when the *P*16 and *P*40 transitions are saturated by the excitation laser.

A Boltzmann plot of ln (I/S) as a function of the energy of the upper rotational levels in the *P* branch of the $B^2\Sigma^+ \rightarrow X^2\Sigma^+(0\text{-}0)$ band of CN probed is shown in Fig. 9. Transitions out of two rotational levels are saturated by the laser and the fluroescence from individual transitions in the *R* branch are detected. Under these conditions the line strengths *S* are equal to $K'+K''+1$. A temperature obtained from the redistribution spectrum, Fig. 9, is consistent with the temperatures obtained by OES and LIF. This indicates that the rotation changing collision rate is large enough to equilibrate the excited rotational levels.

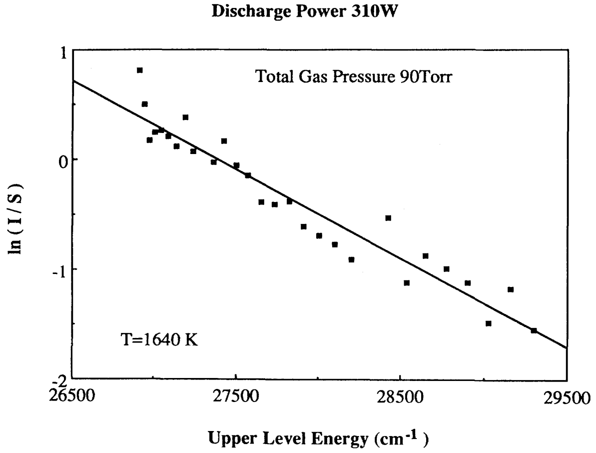

FIG. 9. Rotational temperature obtained using redistributed LIF of the *R* branch in the $B^2\Sigma^+ \rightarrow X^2\Sigma^+$(0-0) band of CN when the *P*16 and *P*40 transitions are saturated by the excitation laser. The total pressure was 90-Torr with CH_4 :H_2=2% by volume. The line strength S is equal to $K'+K''+1$.

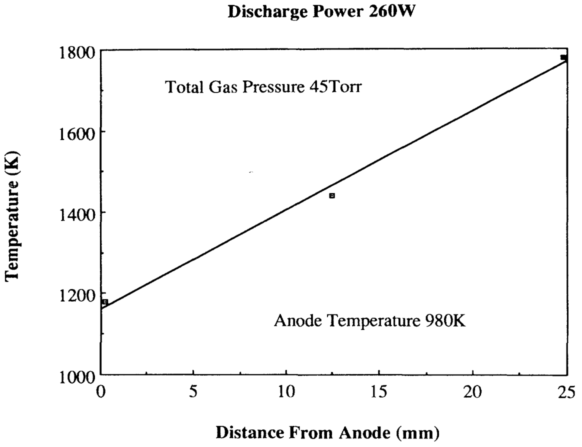

FIG. 11. Gas temperature as a function of spatial position between anode and cathode. The gas temperature was measured using emission intensities of the H_2 molecule at 45-Torr total pressure with CH_4:H_2=1% by volume. The anode was heated to 980 K.

VI. GAS TEMPERATURE SURVEY RESULTS

The gas kinetic temperature in our hollow cathode CH_4-H_2 discharge has been measured as a function of the position in the discharge and the power put into the discharge using the relative line intensities of emission from the R branch of the $G^1\Sigma_g^+ \rightarrow B^1\Sigma_u^+$(0-0) band of H_2. Figure 10 shows the gas kinetic temperatures measured as a function of discharge power. Figure 11 shows the gas kinetic temperature as a function of position in the discharge. It can be seen from Fig. 10 that the gas temperature is a linear function of input power. This is anticipated since one expects that much of the input power is consumed by neutral species in a weakly ionized discharge. Figure 11 shows a linear relation between gas temperature and position in the discharge. This indicates that the heat transfer in our PACVD system is dominated by conduction and radiation instead of thermal convection. If convection is occurring the gas temperature should vary slowly as a function of position except in a thin thermal boundary layer within which the gas temperature varies rapidly. If convection is not dominant, the gas temperature should decrease as a linear function of positions between the walls of a reactor [21]. The measurements shown in Fig. 11 support the latter case. Therefore, we conclude that convection is not the dominant heat-transfer mechanism in our system.

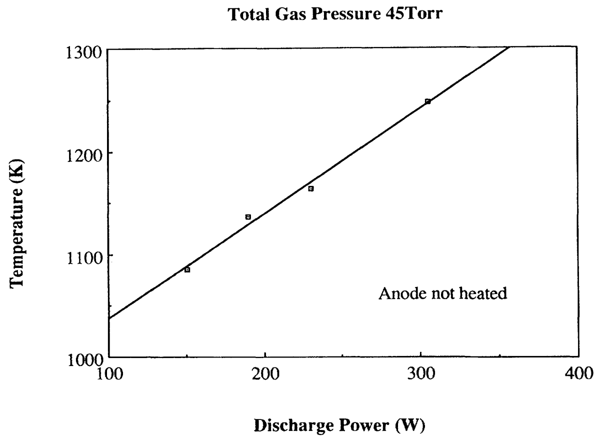

FIG. 10. Gas temperature as a function of input discharge power. The gas temperature was measured using emission intensities of the H_2 molecule at 45-Torr total pressure with CH_4:H_2=1% by volume. Data were taken at a position within 0.5 mm of the anode with no anode heating.

We have attempted to use a thermocouple probe to measure the gas temperature. An invasive probe like this is a significant electrical, thermal, and chemical perturbation to the plasma. Unreasonably high temperatures (6000 K) were obtained from the probe measurment. We suspect that charged particle bombardment and/or surface recombination of atomic hydrogen is heating the probe. Even higher termperatures are obtained if the probe is biased either positively or negatively.

VIII. SUMMARY

Generally neither relative vibrational nor relative electronic level populations are in thermal equilibrum at either the electron or gas kinetic temperature in glow discharges. Relative rotational level populations are determined primarily by rotation changing collisions with neutrals in a glow discharge and hence may be in equilibrium at the gas kinetic temperature at moderate pressure. We note that our measurements give the gas kinetic temperature but not the electron or ion temperatures.

The gas kinetic temperature in a CH_4-H_2 discharge has been measured using OES of both the *R* branch of the $G^1\Sigma_g^+ \rightarrow B^1\Sigma_u^+(0\text{-}0)$ band of H_2 and the *R* branch of the $B^2\Sigma^+ \rightarrow X^2\Sigma^+(0\text{-}0)$ band of CN. These measurements have been confirmed by LIF measurements of the temperature and LIF measurements of rotation changing collisions. The gas temperature varies linearly with the position between the cathode and the anode and with the input discharge power. Optical emission spectroscopy of the *R* branch of the $G^1\Sigma_g^+ \rightarrow B^1\Sigma_u^+(0\text{-}0)$ band of H_2 can be used as a simple and inexpensive technique for obtaining the gas kinetic temperature during plasma assisted chemical-vapor deposition of diamond.

ACKNOWLEDGMENTS

Research supported by the National Science Foundation under Engineering Research Center for Plasma-Aided Manufacturing Grant No. ECD-8721545, the U.S. Army Research Office under Grant No. DAAL03-90-G-0115, and by the Thin Film Deposition and Applications Center of the University of Wisconsin–Madison.

---

[1] K. Suzuki, A. Sawabe, H. Yasuda, and T. Inuzuka, Appl. Phys. Lett. **50**, 728 (1987).

[2] S. Matsumoto, Y. Sato, M. Kamo, and N. Setaka, Jpn. J. Appl. Phys. **21**, L183 (1982).

[3] K. Kurihara, K. Sasaki, M. Kawarada, and N. Konshino, Appl. Phys. Lett. **52**, 437 (1988).

[4] B. Singh, O.R. Mesker, A.W. Levine, and Y. Arie, Appl. Phys. Lett. **52**, 1658 (1988).

[5] K. Kobashi, K. Nishimura, Y. Kawate, and T. Horiuchi, Phys. Rev. B **38**, 4067 (1988).

[6] Y. Liou, A. Inspektor, R. Weimer, and R. Messier, Appl. Phys. Lett. **55**, 631 (1989).

[7] W. L. Hsu, D. M. Tung, E. A. Fuchs, K. F. McCarthy, A. Joshi, and R. Nimmagadda, Appl. Phys. Lett. **55**, 2739 (1989).

[8] H. M. Crosswhite, *The Hydrogen Molecule Wavelength Table of Gerhard Heinrich Dieke* (Wiley, New York, 1972).

[9] G. Herzberg, *Molecular Spectra and Molecular Structure* (Krieger, Malabar, FL, 1989), Vol. I.

[10] G. H. Dieke, J. Mol. Spectrosc. **2**, 494 (1958).

[11] A. T. Wager, Phys. Rev. **64**, 18 (1943).

[12] J. van der Linde, and F. W. Dalby, Can. J. Phys. **50**, 287 (1972).

[13] R. J. Gallagher and J. B. Fenn, J. Chem. Phys. **60**, 3492 (1974).

[14] W. M. Jackson, J. Chem. Phys. **61**, 4177 (1974).

[15] W. M. Jackson and R. J. Cody, J. Chem. Phys. **61**, 4183 (1974).

[16] R. W. B. Pearse and A. G. Gaydon, *The Identification of Molecular Spectra* (Wiley, New York, 1963).

[17] R. S. Mulliken, Rev. Mod. Phys. **3**, 89 (1931).

[18] R. S. Mulliken, Phys. Rev. **36**, 611 (1930).

[19] A. T. Wager, Phys. Rev. **64**, 18 (1943).

[20] K. M. Evenson and H. P. Broida, J. Chem. Phys. **44**, 1637 (1966).

[21] M. Fishenden and O. A. Saunders, *An Introduction to Heat Transfer* (Oxford, London, 1950).